Probability distillation: A caveat and alternatives

Chin-Wei Huang[*1,2] **Faruk Ahmed**[*1] **Kundan Kumar**[1,3] **Alexandre Lacoste**[2] **Aaron Courville**[1,4]
[1]Mila, University of Montreal [2]Element AI [3]Lyrebird.ai [4]CIFAR Fellow
{chin-wei.huang, faruk.ahmed}@umontreal.ca

Abstract

Due to Van den Oord et al. (2018), probability distillation has recently been of interest to deep learning practitioners, where, as a practical workaround for deploying autoregressive models in real-time applications, a student network is used to obtain quality samples in parallel. We identify a pathological optimization issue with the adopted stochastic minimization of the reverse-KL divergence: the curse of dimensionality results in a skewed gradient distribution that renders training inefficient. This means that KL-based "evaluative" training can be susceptible to poor exploration if the target distribution is highly structured. We then explore alternative principles for distillation, including one with an "instructive" signal, and show that it is possible to achieve qualitatively better results than with KL minimization.

1 INTRODUCTION

Deep autoregressive models are currently among the best choices for unsupervised density modeling tasks (Van den Oord et al., 2016b,a). However, due to the factorization induced by such models on the data space by the chain rule of probability, sampling from such models requires $\mathcal{O}(T)$ sequential computation steps, where T is the dimension/sequence-length of the data. This makes sampling slow and inefficient for most practical purposes. A recent solution to alleviating this bottleneck was proposed by Van den Oord et al. (2018), who show that an autoregressive *WaveNet* model (Van den Oord et al., 2016a) can be distilled into a student network, which is significantly faster to sample from due to parallel computation, and therefore much more suitable for deployment in real-time applications.

In this paper, we identify a fundamental issue with the approach taken by Van den Oord et al. (2018), and provide alternative perspectives for distilling the sampling process of a teacher model.

The solution proposed by Van den Oord et al. (2018) is to minimize the reverse Kullback-Leibler divergence (KL) between the student and the teacher distribution. Generally, this relies on two essential components: (1) the gradient signal from the teacher network (the WaveNet model) and (2) invertibility of the student network (the Parallel WaveNet model). This allows samples drawn from the student to be evaluated under the likelihood of both models, and the student can then be updated via stochastic backpropagation from the teacher. The student is implemented with an inverse autoregressive transformation (Kingma et al., 2016) which admits fast sampling at the cost of slow likelihood estimation. On the other hand, since the autoregressive teacher allows fast evalution of likelihoods but is slow to sample from, the approach takes advantage of the best of both worlds.

In theory, it seems that minimizing the KL should be sufficient for distilling a teacher into a student. However, in practice, it has been necessary to implement additional heuristics in order to achieve samples with similar realism as that of the teacher (Van den Oord et al., 2018; Ping et al., 2018). In particular, a *power loss* that biases the power across frequency bands of the student sampler to match that of human speech patterns has been crucial in recent work for generating synthesized speech without the student collapsing to unrealistic "whispering".

Our contributions are as follows.

- We show how the reverse-KL loss is ill-suited for the task of probability distillation. Roughly speaking, this is because the teacher distribution typically possesses a low-rank nature for high-dimensional structured data, making the *expansion signal* (defined in Section 3.1), which is necessary for successfully distilling such a teacher, a rare event.

- We then explore different alternatives for distillation, by recasting the problem of distillation into learning a transformation of probability density from a prior space to the data space. This view connects decoder-based generative models with probability density distillation.

- Finally, we run experiments with images and speech data, demonstrating that it is possible to learn fast samplers with our proposed alternatives, which do not suffer from the pathologies of reverse-KL training.

2 AUTOREGRESSIVE MODELS

Given a joint probability distribution $p(x)$, where x denotes a T-dimensional vector, one can factorize the distribution according to the *chain rule of probability*, for arbitrary ordering of dimensions:

$$\begin{aligned} p(x) &= p(x_1)p(x_2|x_1)...p(x_T|x_1,...,x_{T-1}) \\ &= \prod_{t=1}^{T} p(x_t|x_{1:t-1}) \end{aligned} \tag{1}$$

In the tabular case, i.e. when x_t can take V different possible values, the joint probability can be represented by a table of $\mathcal{O}(V^T)$ entries. When the event set of x_t is uncountable, the joint density is not even tractable. This motivates the use of a parametric model to compress the conditional probability $p(x_t|x_{1:t-1})$, where one has $p_\theta(x) = \prod_{t=1}^{T} p_\theta(x_t|x_{1:t-1})$. This is referred to as an *autoregressive model*. Parameters are usually shared across the dimensions of x, since T may vary, for example in the case of recurrent neural networks or convolutional neural networks, which have been empirically demonstrated to possess good inductive biases for tasks involving images (Van den Oord et al., 2016b) and speech data (Van den Oord et al., 2016a). However, sampling is sequential, requiring T passes, which is why autoregressive models are slow to sample from, making them impractical for tasks requiring sampling, such as speech generation. This has motivated the work of Van den Oord et al. (2018), who propose *probability density distillation* to learn a student network with a structure that allows for parallel sampling, by distilling a state-of-the-art autoregressive teacher into it.

3 PROBABILITY DISTILLATION WITH NORMALIZING FLOWS

Van den Oord et al. (2018) propose to distill the probability distribution parameterized by a WaveNet model (the teacher network, denoted by $\mathcal{T}$) by minimizing its reverse-KL with a student network (denoted by $\mathcal{S}$):

$$D_{\mathrm{KL}}(p_\mathcal{S} \,||\, p_\mathcal{T}) = \mathbb{E}_{x\sim p_\mathcal{S}}[\log p_\mathcal{S}(x) - \log p_\mathcal{T}(x)] \tag{2}$$

The idea is to leverage recent advances in *change of variable* models (also known as *normalizing flows*) (Rezende & Mohamed, 2015; Kingma et al., 2016; Huang et al., 2018a; Berg et al., 2018) to parallelize the computation of the sampling process.

First, the student distribution is constructed by transforming an initial distribution $p_\mathcal{S}(z)$ (e.g. normal or uniform distribution) in a way such that each dimension x_t in the output x depends only on up to t preceding variables (according to a chosen ordering) in the input z:

$$\begin{aligned} z &\sim p_\mathcal{S}(z), \\ x_t &\leftarrow f_t(z_t; \pi_t(z_1, ..., z_{t-1})),\ \forall t, \end{aligned} \tag{3}$$

where f_t is an invertible map between z_t and x_t. Unlike the sampling process of an autoregressive model, where one needs to accumulate all $x_{1:t-1}$ to sample x_t from $p_\mathcal{T}(x_t|x_{1:t-1})$, which scales $\mathcal{O}(T)$, the transformations f_t can be carried out independently of t, allowing for $\mathcal{O}(1)$ time sampling due to the parallel computation.

Second, the entropy term of $p_\mathcal{S}$ can be estimated using the change of variable formula:

$$\mathbb{E}_{x\sim p_\mathcal{S}(x)}[\log p_\mathcal{S}(x)] = \mathbb{E}_{z\sim p_\mathcal{S}}\left[\log p_\mathcal{S}(z) \left|\frac{\partial f(z)}{\partial z}\right|^{-1}\right] \tag{4}$$

where f is the multivariate transformation $f(z)_t \doteq f_t(z_t; z_{<t})$. Furthermore, owing to the partial dependency of f_t, f has a triangular Jacobian matrix, reducing the computation of the log-determinant of the Jacobian in Eq. (4) to linear time:

$$\left|\frac{\partial f(z)}{\partial z}\right| = \prod_t \frac{\mathrm{d} f_t(z_t; z_{<t})}{\mathrm{d} z_t}. \tag{5}$$

Finally, when the teacher network has a tractable explicit density, one can evaluate the likelihood of samples drawn from $p_\mathcal{S}$ under $p_\mathcal{T}$ efficiently (in the case of autoregressive models such as WaveNets, one can use teacher forcing, or equivalently, change of variable formula, to compute log-likelihood in parallel).

3.1 ANALYSIS OF THE CURSE OF DIMENSIONALITY

Assume the student density $p_\mathcal{S}$ lies within a certain family $\mathcal{Q}$. Ideally, if $p_\mathcal{T} \in \mathcal{Q}$, the solution to the minimization problem in Equation (2) would be $p_\mathcal{S} = p_\mathcal{T}$. However, this is not trivial in practice when an oracle solver

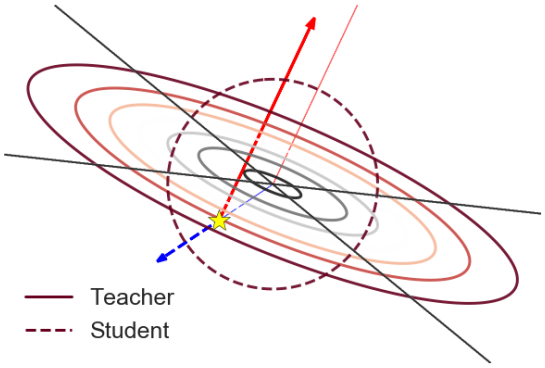

(a) Gradients from teacher (red) and student (blue).

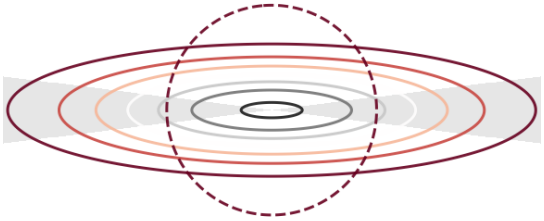

(b) Rotated by eigenvectors of $\Sigma_{\mathcal{T}}$.

Figure 1: When distilling the teacher distribution (red) with a student distribution (blue) by minimizing the KL divergence, the student receives two counteracting gradient signals from the two corresponding likelihood terms. The probability of receiving a signal to expand out the student distribution to fill the teacher is proportional to the relative amount of space occupied by the shaded area, which vanishes when the covariance matrix of the teacher has trivial eigenvalues.

does not exist, forcing us to resort to stochastic optimization to update $p_{\mathcal{S}}$ iteratively. In this section, we identify a failure mode of distillation when stochastically minimizing the reverse-KL with gradient descent.

Empirically, there are two stages during stochastic minimization of the reverse-KL:

(i) $p_{\mathcal{S}}$ starts to fit to the mode of $p_{\mathcal{T}}$, and

(ii) $p_{\mathcal{S}}$ gradually expands from the mode of $p_{\mathcal{T}}$ to fit the shape of the distribution.

Stage (i) is fast due to the well-known zero forcing property of the reverse-KL (Minka et al., 2005). Figure 1.3 of Turner & Sahani (2011) shows that $p_{\mathcal{S}}$ tends to be more concentrated when it is assumed to be fully factorial (independent). We show that even when $\mathcal{Q}$ contains $p_{\mathcal{T}}$, stochastic optimization can be slow in stage (ii) and thus result in a more concentrated, suboptimal $p_{\mathcal{S}}$. This implies it is not only a matter of the assumption on the family of $p_{\mathcal{S}}$, but on how we optimize it.

Intuitively, for each sample x drawn from $p_{\mathcal{S}}$ using reparamerization, the negative gradient of the integrand in Equation (2) with respect to x is made up of two counteracting factors: one that pushes x away from the mode of the student density $p_{\mathcal{S}}$ (max entropy) and one that pulls x towards the mode of the teacher density $p_{\mathcal{T}}$ (min energy). These two counteracting terms form the "error" component of the *path derivative* (Roeder et al., 2017):

$$\nabla_x(\log p_{\mathcal{S}_\phi}(x) - \log p_{\mathcal{T}}(x))\nabla_\phi f_\phi(z),\ x = f_\phi(z), \tag{6}$$

when the student is updated (see Appendix B for more details). Hence, there is an intrinsic exploration-exploitation tradeoff in the nature of this method. We show below that this learning algorithm tends to exploit more: the gradient of a sample x is much more likely to point towards the high density region under the teacher, which means $-\log p_{\mathcal{T}}$ dominates, collapsing the student.

To analyze the efficiency of training with reverse-KL, we consider the case when both the student and teacher are multivariate normal centered at the origin, as a model of the problem. Assume without loss of generality[1] that $p_{\mathcal{S}} = \mathcal{N}(0, \mathbb{I})$ and $p_{\mathcal{T}} = \mathcal{N}(0, \Sigma_{\mathcal{T}})$ (both centered at 0 to analyze the efficiency of stage (ii)), where $\mathbb{I}$ is an n-by-n identity matrix and $\Sigma_{\mathcal{T}} \in S^n_{++}$ is a positive definite matrix.

Let $g_x \doteq \nabla_x(\log p_{\mathcal{T}}(x) - \log p_{\mathcal{S}}(x))$ be the negative gradient *wrt* the random variable $x \sim p_{\mathcal{S}}$. We are interested in the event $\{x^\top g_x > 0\}$, which we call the *expansion signal*, as it denotes the event of the gradient pointing away from the teacher's mode, thereby helping the student expand its probability mass. The following proposition establishes the connection between the eigenvalues of the covariance matrix $\Sigma_{\mathcal{T}}$ and the probability of the expansion signal.

Proposition 1. *Let $p_{\mathcal{S}} = \mathcal{N}(0, \mathbb{I})$ and $p_{\mathcal{T}}(0, \Sigma_{\mathcal{T}})$. Draw $x \sim p_{\mathcal{S}}$. Let A_U be the surface area of the unit sphere $U = \{x : \|x\|_2 = 1\}$, and $A_{U_{\cap\rho}}$ be the surface area*

[1] When the covariance matrix of the student distribution $\Sigma_{\mathcal{S}}$ is not an identity matrix, one can transform both $p_{\mathcal{S}}$ and $p_{\mathcal{T}}$ via the change of variable: $x' = U^{-\top}x$ where $\Sigma_{\mathcal{S}} = U^\top U$ is the Cholesky decomposition of the covariance matrix; such that $p_{\mathcal{S}}(x')$ is standardized, $p_{\mathcal{T}}(x')$ has a "relative" covariance (due to the rotation under $U^{-\top}$), and our analysis carries on.

of $\{x \in U : \sum_i \rho_i x_i^2 > 0\}$. *Then the probability of* $\{x^\top g_x > 0\}$ *is given by*

$$\frac{A_{U_\cap \rho}}{A_U} \tag{7}$$

where $\rho_i = 1 - \frac{1}{d_i^2}$ *and* d_i^2 *is the* i*-th eigenvalue of the covariance matrix.*

Proof. By definition, we have $g_x = -\Sigma_{\mathcal{T}}^{-1} x + x$. Let $\Sigma_{\mathcal{T}} = \Lambda D \Lambda^{-1}$ be the eigen-decomposition of the covariance, where $D_{ii} = d_i^2$ is the i-th eigenvalue and the columns of Λ are the eigenvectors. Due to the rotational invariance and the uniformity of the density of the standard normal $p_{\mathcal{S}}$ on the level set $\{x : \|x\|_2 = r\}$ for any $r > 0$,

$$\begin{aligned}\mathbb{P}\left\{x^\top g_x > 0\right\} &= \mathbb{P}\left\{x^\top \Lambda (\mathbb{I} - D^{-1}) \Lambda^{-1} x > 0\right\} \\ &= \mathbb{P}\left\{\sum_i \left(1 - \frac{1}{d_i^2}\right) x_i^2 > 0\right\} = \frac{A_{U_\cap \rho}}{A_U}.\end{aligned}$$

□

Illustration of the proposition. What the proposition implies is that the chances of receiving a gradient signal that points outward depend on the eigenvalues of the covariance matrix of the teacher: the greater the number of eigenvalues that are smaller than 1 (more ill-conditioned), the lower the chances. This means that the expansion signal via the path derivative can be increasingly unlikely when the dimensionality in x grows and $p_{\mathcal{T}}$ is highly structured. Consider Figure 1a for example, where the solid contour plot and dashed contour plot represent the densities of $p_{\mathcal{T}}$ and $p_{\mathcal{S}}$, respectively. For a random sample drawn from $p_{\mathcal{S}}$, marked by the yellow star, the gradients of $\log p_{\mathcal{T}}$ and $-\log p_{\mathcal{S}}$ with respect to it are represented by the red and blue arrows. The net g_x here can be decomposed into two parts: one that is perpendicular to x, $g_{x,\perp}$, and one that is parallel with x, $g_{x,\|}$. In this example, x and $g_{x,\|}$ point in opposite directions, meaning the back-propagated signal would pull x towards the mode of $p_{\mathcal{T}}$.

Asymptotics of teacher density. On average, the chances of getting a stochastic gradient signal that push the points away from the mode is the fraction of the area of the unit sphere intersecting with the hypercone, represented by the shaded area in Figure 1b. In practice, such a condition coefficient can be very small, as it is well known that a high dimensional distribution over structured data is effectively low-rank. This makes it harder for $p_{\mathcal{S}}$ to expand its probability mass along the high density manifold under $p_{\mathcal{T}}$. In fact, the smallest eigenvalue of a normalized (scaled by $1/T$) Wishart distribution [2] converges almost surely to zero as the dimensionality T approaches infinity (Silverstein et al., 1985). For a more general depiction of the asymptotic distribution of the eigenvalues, see the Marchenko-Pastur Law (Marchenko & Pastur, 1967).

Although our analysis here deals with the Gaussian case for ease of analysis, the theme extends to any degenerate distribution. For realistic data distributions, such as natural images, the data usually lies within low-dimensional manifolds (Carlsson et al., 2008; Fefferman et al., 2016; Narayanan & Mitter, 2010), and our arguments apply generally for such cases.

3.2 EMPIRICAL DEMONSTRATION

We showed above that with increasing dimensionality, and for a structured teacher, there is a diminishing probability of gradient signals that can push the student to expand around the mode of the teacher. We speculate that the distilled density of the student will therefore be collapsed around the mode of the teacher density, resulting in student samples having higher likelihood under the teacher than a "typical" sample drawn from the teacher would normally have. We validate this hypothesis in the following experiment.

We take both $p_{\mathcal{T}}$ and $p_{\mathcal{S}}$ to be multivariate Gaussian distributions, with the sampling process defined as $x \leftarrow \mu + R \cdot z$ where $\mu \in \mathbb{R}^T$, $R \in \mathbb{R}^{T \times T}$ and $z \sim \mathcal{N}(0, \mathbb{I})$. We randomly initialize each element of R for $\mathcal{T}$ independently according to the standard Gaussian, set $\mu = [2, ..., 2]^\top$ to be a vector of T 2's, and fix them while training $\mathcal{S}$ to distill $\mathcal{T}$. For $T \in [4, 16, 32, 64]$, training proceeds as follows: we sample x from the student, estimate $\log p_{\mathcal{S}}(x)$ using the change of variable formula, and evaluate x under $\log p_{\mathcal{T}}$. We use a minibatch size of 64 and learning rate of 0.005 with the Adam optimizer (Kingma & Ba, 2014), and make 5000 updates. For evaluation, we draw 1000 samples from both $p_{\mathcal{T}}$ and $p_{\mathcal{S}}$, and display the empirical distribution of $\log p_{\mathcal{T}}(x)$ in Figure 2a.

First, we observe that the log-likelihood of the teacher samples deviate from 0 as dimensionality grows. In fact, assuming x_t is sampled i.i.d. (for simplicity) from a distribution whose second moment m_2 exists, the l_2 norm of $\bar{x} \doteq \frac{x}{\sqrt{T}}$ would almost surely converge to m_2, by the strong law of large numbers. This is a phenomenon known as the *concentration of measure*. To see this, observe that:

[2] Wishart is the conjugate prior of the precision matrix (inverse of covariance) of a multivariate Gaussian

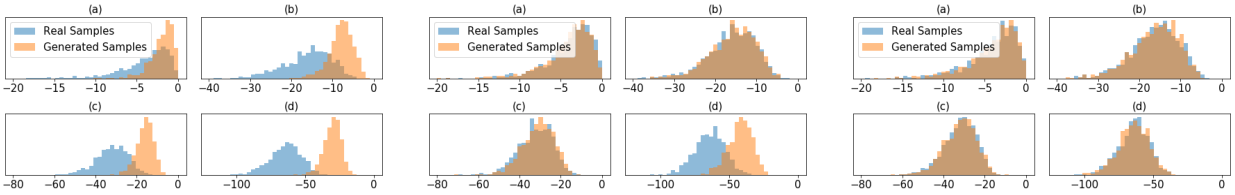

(a) Distillation with KL (b) With z-reconstruction (c) With x-reconstruction

Figure 2: We distill a Gaussian teacher with a Gaussian student. x-axis: likelihood under the teacher; y-axis: count of samples drawn from the teacher (real samples) and the learned student (generated samples). (a-d) in the subfigures correspond to $\{4, 16, 32, 64\}-$ dimensional multivariate Gaussians.

$$\|\bar{x}\|_2^2 = \bar{x}^\top \bar{x} = \sum_{t=1}^{T} \bar{x}_t^2 = \sum_{t=1}^{T} \left(\frac{x_t}{\sqrt{T}}\right)^2 \tag{8}$$

$$= \frac{1}{T} \sum_{t=1}^{T} x_t^2 \longrightarrow m_2, \quad \text{a.s. as } T \to \infty. \tag{9}$$

The concentration is due to the compromise between density and volume of space (which vanishes exponentially as dimensionality grows). The consequence is that when one samples from a high dimensional Gaussian, the norm of the sample can be well described a constant, which means one is effectively sampling from the shell of the Gaussian ball.

Second, with an increasing number of dimensions, we observe that $p_{\mathcal{S}}$ does indeed concentrate more on the high density region of $p_{\mathcal{T}}$. This suggests that the imbalanced gradient signal poses an optimization problem for distillation of higher dimensional structured distributions. To validate this, we repeat the experiment 8 times, and estimate the probability of the gradient signal pointing away from the mode of the teacher throughout training of the student by drawing 128 samples at each time step (averaging out all 1,024 binary values).

The resulting plots are shown in Figure 3. The sudden increase in the probability at the initial stage indicates that the student quickly fits to and concentrate around the mode of the teacher, as per stage (i). After the student expands to a reasonable size and shape, per stage (ii), the probablity drops and getting an expansion signal along the thin manifold under the teacher density becomes increasingly unlikely as dimensionality grows, which is consistent with Proposition 1.

Additionally, the mismatch of norm (after centering, i.e. likelihood) in Figure 2a implies that the use of KL would result in a mismatch of certain important statistics (such as norm of the samples, which is a perceivable feature in images and audio frames) even when $p_{\mathcal{S}}$ is fairly close to $p_{\mathcal{T}}$.

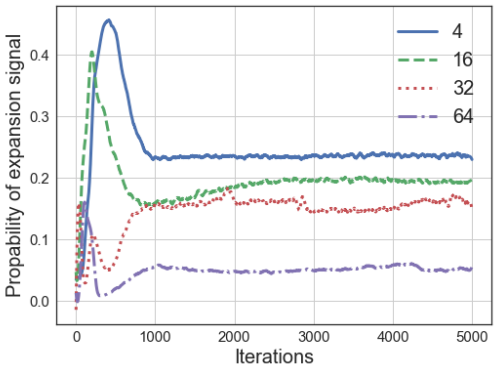

Figure 3: Estimate of probability of expansion signal throughout training of the student (with reverse-KL loss). The legend indicates the dimensionality of the problem.

Finally, in the above study, we only identify this optimization difficulty in the case of Gaussian teacher and Gaussian student. However, it is also well known that the reverse-KL tends to be mode-seeking (see Figure 4b,4c for example), and is not well-suited for learning multimodal densities (Turner & Sahani, 2011; Huang et al., 2018b).

4 PROBABILITY DISTILLATION WITH *INVERSE MATCHING*

In this section, we discuss possible alternatives for distilling a teacher. We assume there exists an invertible mapping from a prior space $\mathcal{Z}$ to the data space $\mathcal{X}$, such that one can trivially sample from a prior distribution $z \sim p_{\mathcal{T}}(z)$ and pass the sample through this invertible map such that the sample is distributed according to $p_{\mathcal{T}}(x)$. For Gaussian conditional autoregressive models, for example, one would sequentially pass scalar standard Gaussian noise z_t through the following recursive function $x_t = \mu_t(x_{1:t-1}) + \sigma_t(x_{1:t-1}) \cdot z_t$. For notational convenience, we denote the "inverse" of this transforma-

tion by $\mathcal{T} : \mathcal{X} \to \mathcal{Z}$, as this is the inverse autoregressive transformation that can be parallelized. The goal is to learn the sampling transformation, i.e. $\mathcal{T}^{-1}$. Similarly, we define the forward pass of the student as the mapping $\mathcal{S} : \mathcal{Z} \to \mathcal{X}$.

Ideally, since the transformation is deterministic, it's most natural to simply minimize the prediction loss according to some distance metric $d(\mathcal{T}^{-1}(z), \mathcal{S}(z))$, where $z \sim p_{\mathcal{T}}(z)$. When this loss function equals zero almost everywhere, passing the prior sample through $\mathcal{S}$ would induce an identical distribution as $p_{\mathcal{T}}$. We refer to this setup as **distillation with oracle prediction**. However, preparing such a dataset of $\mathcal{T}^{-1}(z)$ samples would typically be time-consuming. We present the following two alternatives.

1. Distillation with z-reconstruction. We consider minimizing $d(z, \mathcal{T} \circ \mathcal{S}(z))$, which is a reconstruction loss and the student network and teacher network are viewed as the encoder and decoder, respectively. In this case, since $\mathcal{T}$ is invertible and fixed, the only functional form of $\mathcal{S}$ that gives zero reconstruction would be $\mathcal{T}^{-1}$, which means the random variable $\mathcal{S}(Z)$ should also be distributed according to $p_{\mathcal{T}}$. In fact, minimizing the z-reconstruction loss corresponds to a parametric distance induced by the teacher network. Define $d_{\mathcal{T}}(a, b) \doteq d(\mathcal{T}(a), \mathcal{T}(b))$, where d is a distance metric. Then

$$\begin{aligned} d_{\mathcal{T}}(\mathcal{T}^{-1}(z), \mathcal{S}(z)) &= d(\mathcal{T} \circ \mathcal{T}^{-1}(z), \mathcal{T} \circ \mathcal{S}(z)) \\ &= d(z, \mathcal{T} \circ \mathcal{S}(z)). \end{aligned}$$

Interestingly, $d_{\mathcal{T}}$ is also a metric:

Proposition 2. *$d_{\mathcal{T}}$ is a metric if and only if $\mathcal{T}$ is injective.*

Proof. Trivially, positive-definiteness and symmetry are inherited from d if and only if $\mathcal{T}$ is an injection. To see that subadditivity is also preserved, for some a, b and c, let $\mathcal{T}_a = \mathcal{T}(a)$, $\mathcal{T}_b = \mathcal{T}(b)$ and $\mathcal{T}_c = \mathcal{T}(c)$. Since $d(\mathcal{T}_a, \mathcal{T}_b) \leq d(\mathcal{T}_a, \mathcal{T}_c) + d(\mathcal{T}_b, \mathcal{T}_c)$, due to the subadditivity of d, for any $\mathcal{T}_a$, $\mathcal{T}_b$ and $\mathcal{T}_c$, we have $d_{\mathcal{T}}(a, b) \leq d_{\mathcal{T}}(a, c) + d_{\mathcal{T}}(b, c)$ for any a, b and c. □

This means that the z-reconstruction loss behaves like a distance between $\mathcal{T}^{-1}(z)$ and $\mathcal{S}(z)$. So when z-reconstruction is minimized, it implies $\mathcal{S}$ gets closer to $\mathcal{T}^{-1}$ in the sense of the induced (parametric) metric $d_{\mathcal{T}}$. However, this parametric metric is not necessarily good, which we will demonstrate empirically in Section 4.1. A potential failure mode for it is when the teacher has extremely high uncertainty, e.g. large standard deviation for the conditional gaussian distribution, which would result in an inverse mapping (scaled by $1/\sigma$) with an extremely small slope.

2. Distillation with x-reconstruction. Finally, we consider minimizing the reconstruction loss $d(x, \mathcal{S} \circ \mathcal{T}(x))$, where $x \sim p_{\mathcal{D}}$, the (empirical) data distribution, treating the teacher network as the encoder, and the student network as the decoder. When the teacher density coincides with the underlying data distribution, this would be equivalent to training with oracle prediction, as $\mathcal{T}(X)$ would be distributed according to $p_{\mathcal{T}}(z)$. This is a reasonable assumption when $p_{\mathcal{T}}$ approximates $p_{\mathcal{D}}$ well, and this is in fact true as $p_{\mathcal{T}}$ is usually trained with maximum likelihood under $p_{\mathcal{D}}$. This training criterion is more "instructive" in the sense that the student network is shown what a typical sample looks like, whereas both reverse-KL and z-reconstruction rely on "evaluating" the samples drawn from the student network, and then correcting the student based on the (possibly imperfectly calibrated) score assigned by the teacher. Hence, x-reconstruction does not suffer from the exploration problem intrinsic to the evaluative training of reverse-KL minimization and z-reconstruction.

Now we revisit the two essential components required for distillation with reverse-KL.

1. **Invertibility**: None of the three training criteria we explored involves estimating the entropy of $p_{\mathcal{S}}$, so in principle, we do not require invertibility of the student. In fact the entropy of $p_{\mathcal{S}}$ is implicitly maximized since $\mathcal{T}$ is bijective. To prevent degenerate $p_{\mathcal{S}}$, one simply needs to avoid using hidden units of dimensionality smaller than the input size without skip connectivity, which compresses the noise.
2. **Differentiability**: For distillation with oracle prediction and x-reconstruction, we only require the translation between $\mathcal{X}$ and $\mathcal{Z}$, via $\mathcal{T}$ and $\mathcal{T}^{-1}$, which is readily accessible for many standard distributions, e.g. linear map between Gaussians (both $\mathcal{T}$ and $\mathcal{T}^{-1}$), logistic-linear map from mixture of logistics to uniform ($\mathcal{T}$ only, but sampling is achievable by sampling the mixture component first), and neural transformation (Huang et al., 2018a) ($\mathcal{T}$ only). We also note that it is possible to recover uniform density from discrete data, by injecting noise proportional to the probability per class to break ties when passing the data through the cumulative sum of the probability (CDF).

4.1 EXPERIMENTS

4.1.1 Linear model with increasing dimensionality

We replicate the experiment in Section 3.2 with z-reconstruction and x-reconstruction loss (equivalent to oracle prediction in this case). Mapping $\mathcal{T}$ from $\mathcal{X}$ to $\mathcal{S}$ is simply inverse of the sampling transformation. In Figure 2, we observe that both models outperform distil-

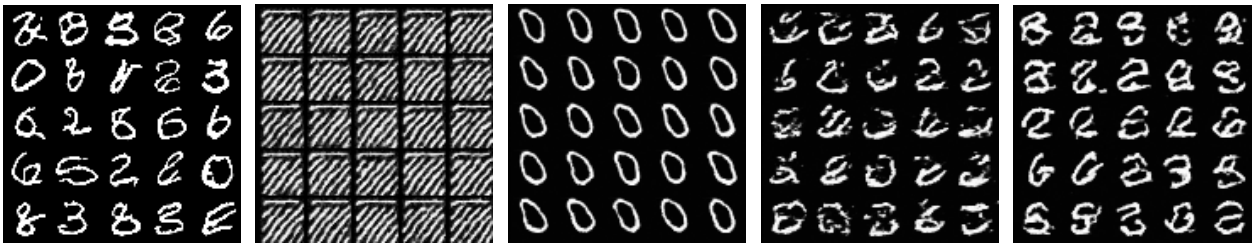

(a) $\mathcal{T}^m$ (b) $\mathcal{S}^m_{KL}$ (c) $\mathcal{S}^m_z$ (d) $\mathcal{S}^m_x$ (e) $\mathcal{S}^m_O$

(f) $\mathcal{T}^f$ (g) $\mathcal{S}^f_{KL}$ (h) $\mathcal{S}^f_z$ (i) $\mathcal{S}^f_x$ (j) $\mathcal{S}^f_O$

Figure 4: Density distillation of teacher models trained on MNIST (first row) and Fashion-MNIST(second row). *Column 1*: samples from teacher network $\mathcal{T}$. *Column 2*: samples from student trained with the KL loss $\mathcal{S}_{KL}$. *Column 3*: samples from student trained with the z-reconstruction loss $\mathcal{S}_z$. *Column 4*: samples from student trained with the x-reconstruction loss $\mathcal{S}_x$. *Column 5*: samples from student trained with the x-reconstruction loss where x is sampled from the teacher $\mathcal{S}_O$.

(a) l_2 reconstruction (b) l_1 reconstruction (c) l_2, noise (d) l_1, noise (e) $(l_2 + l_1)/2$, noise

Figure 5: Experiments with a ResNet student using (a) l_2 x-reconstruction loss, (b) l_1 x-reconstruction loss, (c) adding $N(0, 0.5)$ noise to the encodings z and using l_2 x-reconstruction loss, (d) adding $N(0, 0.5)$ noise to z and using l_1 x-reconstruction loss, and (e) adding $N(0, 0.5)$ noise to z and using a mixed loss $l_2 + l_1$. In general, we observe that adding noise significantly improves sample quality, and training with l_1 losses lead to sharper samples.

lation with reverse-KL, since likelihood of samples (under the teacher) drawn from them follow more closely the shape of the empirical distribution of likelihood of samples drawn from the teacher. It is worth noting that z-reconstruction also starts to fail with an increasing number of dimensions, suggesting that it might be subject to poor gradient signal if the transformation $\mathcal{T}$ is more complex; we elaborate more on this in the next section. On the other hand x-reconstruction is quite robust to dimensionality (and potentially complexity) of the underlying distribution.

4.1.2 Distillation with different losses

In this section, we distill PixelCNN++ (Salimans et al., 2017) teacher networks trained on the MNIST handwritten digits dataset (LeCun et al., 1998) and the Fashion-MNIST dataset (Xiao et al., 2017). We trained the teacher model for 100 epochs and distilled it into the student with another 100 epochs of updates, using mini-batch size of 64, learning rate of 0.0005 for the Adam optimizer with a decay rate of 0.95 per epoch, 3 ResNet blocks per downsampling and upsampling convolution, 32 hidden channels, and a single Gaussian conditional. The data is preprocessed with uniform noise between pixel values and rescaled using the logit function. We use l_2 loss for the reconstruction and prediction methods.

First, we observe that when trained with the reverse-KL loss, the students collapse on undesirable modes. As shown in (Figure 4b), the inductive bias of the causal convolution leads to higher density of the samples with striped textures. When trained with the z-reconstruction loss, the MNIST student samples all collapse to the same

Figure 6: *(left)* Teacher samples with a PixelCNN on CIFAR-10, *(right)* Student samples using x-reconstruction under the l_1 loss, with noise injection.

digit. Interestingly, when we visualize the corresponding $\mathcal{T}^{-1}(z)$ as we slightly perturb the norm of z (see Appendix A), we observe that the digits abruptly change identity. This suggests that when moving onto a different sublevel set of norm in z-space, the corresponding x jumps from one digit manifold to another, and the direction of z does not preserve digit identity. This might explain why the student collapses to a digit: this is due to the bad local minimum that corresponds to relatively low reconstruction cost in the z-space.

Next, we observe that the student trained with x-reconstruction loss (Figure 4d) does not have good quality samples while the reconstructions are visually perfect. We hypothesize this is due to the well-known problem of mismatch between the empirical distribution of the encodings $\mathcal{T}(x)$ and the prior distribution $p_S(z)$ of training decoder based generative models (Kingma et al., 2016). We contrast this with a student trained on oracle predictions (Figure 4e) and observe that the latter's samples match the teacher's samples better.

Finally, we see that the samples from the teacher trained on Fashion-MNIST with the x-reconstruction loss (Figure 4i) have a smoother texture than the one trained with oracle samples (Figure 4j), which again, are perceptually closer to samples from the teacher. We elaborate more on this discrepancy in the next section.

4.1.3 Learning to distill and learning to generate

Since we are not constrained in our modeling choice for the student, we experiment with a ResNet student which is trained to directly map an encoded datapoint from the teacher back to the datapoint. The ResNet is deep enough so that the receptive field at the output is sufficient to span all of the encoded z, so that far-away influence is still exploitable.

Using the l_1 reconstruction cost leads to sharper samples from the student (contrast 5a with 5b). It appears to us that the l_2 loss tends to maintain global details, while the l_1 loss can sometimes sacrifice global coherence for local structure, potentially due to the sparsity induced by it. In 5e, we use an average of both losses in an attempt to maintain both these characteristics, but we notice evidence of the failings manifesting to some extent as well.

A significant improvement in sample quality is observed upon adding Gaussian noise to the encodings before training the student (contrast 5a,5b with 5c,5d). Our intuition for this is as follows: providing a decoder network with pairs of points in the data space and the corresponding encoded (or latent) space would typically result in z-space not being sampled almost everywhere, since image data (and therefore the corresponding encoding in z-space) usually lies on a lower-dimensional manifold, as discussed earlier. Adding noise enhances the support of the distribution, effectively spreading the "responsibility" of an encoding to cover more volume, which smoothens the mapping learned by a decoder. When the goal is to sample from a prior, training methods that encourage such z-space-filling strategies and smoother mappings improve sample quality, which is reminiscent of decoder-based sampling models such as variational auto-encoders (Kingma & Welling, 2014).

This leads us to an important point about these experiments: since the student is trained on noised (encoded) points from the data distribution, this is no longer purely density distillation. The student no longer aims to reproduce the sampling behavior of the teacher (as in 4e), but rather uses the teacher to provide structural information through its encodings. This information, when "spread out" through noise-injection and used by a student to learn decodings into real data (through a reconstruction penalty or more sophisticated losses) results in a network that can now be considered as a stand-alone generator, with the teacher acting as an inference machine that preserves information in the latent space. This can potentially allow a student to outperform its teacher in terms of sample quality, by enabling the learning of a smoother mapping from z-space to data space.

As a demonstration on more realistic data, we train a PixelCNN on CIFAR-10 and distill it with a ResNet student using x-reconstruction with the l_1 loss, and noise injection (Figure 6). We observe that the student learns the desired sampling behaviour, and additionally, owing to the more instructive training with data samples, there is greater global coherence in the samples as compared to the teacher. There is an obvious relative lack of low-level precision, but we believe this comes primarily from the pixel-position uncertainty induced by the pixelwise loss, and could potentially be fixed by augmentating the loss with sophisticated image priors (Ulyanov et al., 2018).

4.1.4 Neural vocoder

Finally, we compare distillation with x-reconstruction and distillation with reverse-KL on the *neural vocoder* task for speech synthesis (Sotelo et al., 2017). The neural vocoder has been an essential component of many text-to-speech models proposed recently (Wang et al., 2017; Shen et al., 2018; Arik et al., 2017; Ping et al., 2018). We train our teacher to map vocoders (Morise et al., 2016) to raw audio using the SampleRNN model (Mehri et al., 2016). We model the conditional distribution of the teacher with a unimodal Gaussian distribution, which makes it easy to compute the corresponding z. We specifically compare against closed form regularized KL with Gaussian conditionals as proposed in Ping et al. (2018). We design our student network with a WaveNet architecture consisting of six flows, and perform sampling as in Parallel WaveNet (Van den Oord et al., 2018). Each flow is a dilated residual block of 10 layers with a convolution kernel width of 2, and 64 output channels. With the x-reconstruction method under an l_1 loss, we find that our student produces samples without the characteristic whispering of the reverse-KL trained student. We have uploaded samples for comparison at `https://soundcloud.com/inverse-matching/sets/samples-for-inverse-matching`.

5 CONCLUSION

In this paper, we investigated problems with distilling an autoregressive generative model under a reverse-KL cost between the student and the teacher, where the student can perform efficient parallel generation. Specifically, we showed that distillation with the reverse-KL can suffer from imbalanced gradient signals due to the curse of dimensionality, making the expansion signal necessary for efficient exploration unlikely. Further, we explored different alternatives which work qualitatively better when compared against distillation with reverse-KL.

ACKNOWLEDGEMENTS

Chin-Wei would like to thank Shawn Tan, and Kris Sankaran for discussion and feedback, and David Krueger for contributing to the idea of minimizing z-reconstruction for distillation.

This work was enabled by the computational resources provided by Compute Canada, Element AI, and Lyrebird.

References

Sercan Arik, Gregory Diamos, Andrew Gibiansky, John Miller, Kainan Peng, Wei Ping, Jonathan Raiman, and Yanqi Zhou. Deep voice 2: Multi-speaker neural text-to-speech. *arXiv preprint arXiv:1705.08947*, 2017.

Rianne van den Berg, Leonard Hasenclever, Jakub M Tomczak, and Max Welling. Sylvester normalizing flows for variational inference. In *Uncertainty in Artificial Intelligence*, 2018.

Gunnar Carlsson, Tigran Ishkhanov, Vin de Silva, and Afra Zomorodian. On the local behavior of spaces of natural images. *International Journal of Computer Vision*, 76(1):1–12, Jan 2008.

Charles Louis Fefferman, Sanjoy Mitter, and Hariharan Narayanan. Testing the manifold hypothesis. *Journal of the American Mathematical Society*, 29(4):983–1049, 10 2016. ISSN 0894-0347. doi: 10.1090/jams/852.

Chin-Wei Huang, David Krueger, Alexandre Lacoste, and Aaron Courville. Neural autoregressive flows. In *International Conference on Machine Learning*, 2018a.

Chin-Wei Huang, Shawn Tan, Alexandre Lacoste, and Aaron Courville. Improving explorability in variational inference with annealed variational objectives. *arXiv preprint arXiv:1809.01818*, 2018b.

Diederik P Kingma and Jimmy Ba. Adam: A method for stochastic optimization. In *International Conference on Learning Representations*, 2014.

Diederik P Kingma and Max Welling. Auto-encoding variational bayes. In *International Conference on Learning Representations*, 2014.

Diederik P Kingma, Tim Salimans, Rafal Jozefowicz, Xi Chen, Ilya Sutskever, and Max Welling. Improved variational inference with inverse autoregressive flow. In *Advances in Neural Information Processing Systems*, pp. 4743–4751, 2016.

Yann LeCun, Léon Bottou, Yoshua Bengio, and Patrick Haffner. Gradient-based learning applied to document recognition. *Proceedings of the IEEE*, 86(11):2278–2324, 1998.

Vladimir Alexandrovich Marchenko and Leonid Andreevich Pastur. Distribution of eigenvalues for some sets of random matrices. *Matematicheskii Sbornik*, 114(4): 507–536, 1967.

Soroush Mehri, Kundan Kumar, Ishaan Gulrajani, Rithesh Kumar, Shubham Jain, Jose Sotelo, Aaron Courville, and Yoshua Bengio. Samplernn: An unconditional end-to-end neural audio generation model. *arXiv preprint arXiv:1612.07837*, 2016.

Tom Minka et al. Divergence measures and message passing. Technical report, Technical report, Microsoft Research, 2005.

Masanori Morise, Fumiya Yokomori, and Kenji Ozawa. World: a vocoder-based high-quality speech synthesis system for real-time applications. *IEICE TRANSACTIONS on Information and Systems*, 99(7):1877–1884, 2016.

Hariharan Narayanan and Sanjoy Mitter. Sample complexity of testing the manifold hypothesis. In J. D. Lafferty, C. K. I. Williams, J. Shawe-Taylor, R. S. Zemel, and A. Culotta (eds.), *Advances in Neural Information Processing Systems 23*, pp. 1786–1794. 2010.

Wei Ping, Kainan Peng, and Jitong Chen. Clarinet: Parallel wave generation in end-to-end text-to-speech. *arXiv preprint arXiv:1807.07281*, 2018.

Danilo Jimenez Rezende and Shakir Mohamed. Variational inference with normalizing flows. In *International Conference on Machine Learning*, 2015.

Geoffrey Roeder, Yuhuai Wu, and David Duvenaud. Sticking the landing: An asymptotically zero-variance gradient estimator for variational inference. In *Advances in Neural Information Processing Systems*, 2017.

Tim Salimans, Andrej Karpathy, Xi Chen, and Diederik P Kingma. Pixelcnn++: Improving the pixelcnn with discretized logistic mixture likelihood and other modifications. In *International Conference on Learning Representations*, 2017.

Jonathan Shen, Ruoming Pang, Ron J Weiss, Mike Schuster, Navdeep Jaitly, Zongheng Yang, Zhifeng Chen, Yu Zhang, Yuxuan Wang, Rj Skerrv-Ryan, et al. Natural tts synthesis by conditioning wavenet on mel spectrogram predictions. In *2018 IEEE International Conference on Acoustics, Speech and Signal Processing (ICASSP)*, pp. 4779–4783. IEEE, 2018.

Jack W Silverstein et al. The smallest eigenvalue of a large dimensional wishart matrix. *The Annals of Probability*, 13(4):1364–1368, 1985.

Jose Sotelo, Soroush Mehri, Kundan Kumar, Joao Felipe Santos, Kyle Kastner, Aaron Courville, and Yoshua Bengio. Char2wav: End-to-end speech synthesis. 2017.

Richard E Turner and Maneesh Sahani. Two problems with variational expectation maximisation for time-series models. *Bayesian Time series models*, 1(3.1): 3–1, 2011.

Dmitry Ulyanov, Andrea Vedaldi, and Victor Lempitsky. Deep image prior. In *Proceedings of the IEEE Conference on Computer Vision and Pattern Recognition*, pp. 9446–9454, 2018.

Aäron Van den Oord, Sander Dieleman, Heiga Zen, Karen Simonyan, Oriol Vinyals, Alex Graves, Nal Kalchbrenner, Andrew W Senior, and Koray Kavukcuoglu. Wavenet: A generative model for raw audio. In *SSW*, pp. 125, 2016a.

Aaron Van den Oord, Nal Kalchbrenner, and Koray Kavukcuoglu. Pixel recurrent neural networks. In *International Conference on Machine Learning*, 2016b.

Aaron Van den Oord, Yazhe Li, Igor Babuschkin, Karen Simonyan, Oriol Vinyals, Koray Kavukcuoglu, George van den Driessche, Edward Lockhart, Luis C Cobo, Florian Stimberg, et al. Parallel wavenet: Fast high-fidelity speech synthesis. In *International Conference on Machine Learning*, 2018.

Yuxuan Wang, RJ Skerry-Ryan, Daisy Stanton, Yonghui Wu, Ron J Weiss, Navdeep Jaitly, Zongheng Yang, Ying Xiao, Zhifeng Chen, Samy Bengio, et al. Tacotron: A fully end-to-end text-to-speech synthesis model. *arXiv preprint*, 2017.

Han Xiao, Kashif Rasul, and Roland Vollgraf. Fashion-mnist: a novel image dataset for benchmarking machine learning algorithms. *arXiv preprint arXiv:1708.07747*, 2017.